Tsunamis Generated by Eruptions from Mount St. Augustine Volcano, Alaska

Jürgen Kienle, Zygmunt Kowalik, T. S. Murty

During an eruption of the Alaskan volcano Mount St. Augustine in the spring of 1986, there was concern about the possibility that a tsunami might be generated by the collapse of a portion of the volcano into the shallow water of Cook Inlet. A similar edifice collapse of the volcano and ensuing sea wave occurred during an eruption in 1883. Other sea waves resulting in great loss of life and property have been generated by the eruption of coastal volcanos around the world. Although Mount St. Augustine remained intact during this eruptive cycle, a possible recurrence of the 1883 events spurred a numerical simulation of the 1883 sea wave. This simulation, which yielded a forecast of potential wave heights and travel times, was based on a method that could be applied generally to other coastal volcanos.

Tsunamis are large water waves that are induced by sudden upheaval or subsidence of the sea floor by an earthquake, submarine landslide, or volcanic explosion. They can travel across the sea over long distances and can be profoundly hazardous, often arriving unexpectedly, far from the source. Tsunamis of volcanic origin have killed a quarter of the people who have died because of the direct effects of catastrophic eruptions that have occurred since A.D. 1000 (*1*). The 1883 eruption of Krakatau in Indonesia was the worst of these disasters (*2*).

Progress toward a firm understanding of how volcanic processes can trigger tsunamis has been slow because few modern field observations are available to study the problem of wave generation, propagation, and run-up. We have studied the case of Mount St. Augustine, an uninhabited island volcano in Lower Cook Inlet, Alaska, which has had six major eruptions since 1778. At least one of these eruptions has demonstrated the potential for the volcano to generate tsunamis. A sea wave accompanied the 6 October 1883 activity and nearly destroyed English Bay, a small coastal community lying 85 km east of the volcano (Fig. 1, top). During the most recent eruption in the spring of 1986, concern for the people and property on the now more populated shores of Cook Inlet led us to do a numerical modeling of the 1883 tsunami. By modeling this event we can check the validity of the models against actual observations of wave arrival time and wave heights at one point on the eastern Lower Cook Inlet shoreline, English Bay. Calibration of the 1883 tsunami also allows the calculation of amplitudes and arrival times of the tsunami at other critical points around Cook Inlet. The models confirmed both the suspected debris-avalanche origin of the tsunami and the risk to communities along the inlet in case of similar future events.

We present in this article the principal results of the models which, in spite of their site-specific nature, could be useful for hazard evaluation at many other sites where an island or coastal volcano is located within an estuary.

Tsunamis Originating at Volcanos

Tsunamis of volcanic origin are caused by a variety of phenomena. Latter (*1*) recognized ten different types of volcanic processes that can generate tsunamis; among the most destructive is large-scale gravitational failure of the volcanic edifice. The collapsing material is incorporated in fast-moving voluminous debris avalanches that leave horseshoe-shaped depressions at the volcano's summit (*3*). Debris avalanches can reach velocities in excess of 100 m/sec (*4*). When a debris avalanche sweeps into the sea, the displaced water mass rushes outward as a tsunami.

Tsunamis pose a risk to populations living along coastal regions, even if the volcano is located several tens of kilometers inland, because of the high mobility of debris avalanches. Siebert *et al.* (*4*) assembled data on nearly 200 Quaternary volcanic debris avalanches and found that some exceeded 20 km^3 in volume and traveled as far as 50 to 100 km from the source. Probable travel distances for small avalanches with volumes of 0.1 to 1 km^3 are between 6 and 11 times the vertical drop. For large avalanches with volumes exceeding 1 km^3, the travel distance can be 8 to 20 times the vertical drop. The mean distance-to-height ratios for these two avalanche classes are 8 and 11, respectively. For example, a debris avalanche originating at a rather small 2000-m-high volcano could be expected to travel as far as 16 to 22 km from the source, depending on the volume of the avalanche. The distance would be much farther if the volcano is higher.

The high population density along Japan's shorelines prompted Japanese observers to keep careful records of tsunamis over the years. Several disastrous tsunamis caused by debris avalanches have been documented in that country (*3*). The worst catastrophe occurred on 21 May 1792 at the Unzen volcanic complex in Kyushu, when simple gravitational collapse of the Mayu-yama lava dome (850 m high) with no accompanying explosive volcanic activity resulted in a 0.34-km^3 debris avalanche that swept into the Ariake Sea, creating hundreds of new islands (*4*). The avalanche overrode the ancient castle town of Shimabara and traveled 6.5 km from its origin. The ensuing tsunami swept 77 km of the Shimabara Peninsula coastline, killing 9528 people, and then traveled 15 km across the Ariake Sea into the Higo and Amakusa provinces, claiming another 4996 lives there. Some 5972 houses were swept away, and more than 1650 ships were destroyed in waves that ran up 10 m along the Shimabara Peninsula and 6 m in the Kumamoto province across the Ariake Sea (*3, 4*). Aida (*5*) developed a

J. Kienle is a professor in the Geophysical Institute and Z. Kowalik is an associate professor in the Institute of Marine Science, at the University of Alaska–Fairbanks, Fairbanks, AK 99775-0800. T. S. Murty is a senior research scientist in the Institute of Ocean Sciences, Sidney, British Columbia V8L 4B2, Canada.

numerical finite-difference model of the tsunami, which was constrained by the historical inundation record.

For more recent eruptions, Krakatau, in 1883, is the only eruption for which good information exists on the timing of explosions and wave arrivals at modern tide gage stations. The tsunamis generated during the course of the eruption reached wave heights of 41 m, and at least 36,417 people living along the shores of the Sunda Straits lost their lives (*2*). Casualties were reported from the Sumatra and Java coasts as far as 120 km from Krakatau. The tsunami-generating mechanism at Krakatau is not straightforward, and various wave generation models have been proposed, including a submarine explosion, edifice collapse resulting in a debris avalanche, and emplacement of a massive bank of pyroclastic debris on the water from a collapsing eruption column (*6*). Numerical modeling of the Krakatau tsunamis has not been attempted yet, although it might be the only way to resolve the nature of the wave-generating mechanism.

Mount St. Augustine

In this article we discuss a hydrodynamic numerical model of a tsunami that was evidently generated by collapse of the edifice of a small, 1200-m-high andesitic-dacitic volcano in the eastern Aleutian arc in Alaska, Mount St. Augustine.

Mount St. Augustine is a young, postglacial, symmetrical island volcano in Kamishak Bay in Lower Cook Inlet, 285 km southwest of Anchorage and 100 km west-southwest of Homer on the Lower Kenai Peninsula (Fig. 1, top). The channel separating the island from the west shore of Cook Inlet is 10 km wide at its narrowest point. The uninhabited, circular island has a diameter of about 12 km, and a single symmetrical volcanic cone rises from its center. The nearest population centers are on the Kenai Peninsula, 100 km to the east, and at Iliamna Lake, 90 km to the northwest.

This volcano has had six significant eruptions since Captain James Cook discovered and named it on 26 May 1778 (St. Augustine's Day). Major eruptions occurred in 1812, 1883, 1935, 1963–64, 1976, and 1986, each dramatically modifying the volcanic edifice. Curiously, the repose times have shortened from 71 years to 52, to 28, to 12, to 10 years for these six historic eruptions (*7, 8*). The highly explosive nature of Mount St. Augustine's eruptions and their short recurrence rate make it the most hazardous volcano in the eastern Aleutian arc and also in the most populous part of Alaska.

The volcano consists of an apron of volcaniclastic deposits and a central complex of dome and dome remnants; lava flows are rare. Mount St. Augustine lavas are predominantly andesitic (57–63% silica) with minor dacite and basalt (*9*). Eruptions are typically less than 0.5 km^3 in volume (dense magma equivalent) and resemble those of Mount St. Helens, Washington, in chemistry and explosivity.

The 1883 Tsunami of Mount St. Augustine

The sudden displacement of a large volume of seawater from the impact of a debris avalanche at the north shore of St. Augustine Island apparently triggered a tsunami on the morning of 6 October 1883. The daily logs that were kept by the Alaska Commercial Company at Alexandrovsky (English Bay) noted (*10, 11*),

> At this morning at 8.15 o'clock 4 Tidal waves flowed with a westerly current, one following the other at the Rate of 30 miles p. hour into the shore, the sea rising 20 feet above the usual Level. At the same time the air became black and foggy, and it began to thunder. With this at the same time it began to rain a finely Powdered Brimstone Ashes, which lasted for about 10 Minutes, and which covered all the parts of Land and everything to a depth of over 1/4 of a inch, clearing up at 9 o'clock A.M. Cause of occurrence: Eruption of the active volcano at the Island of Chonoborough.

Davidson (*12*) vividly described the events of 6 October in a paper published in an early issue of *Science*. According to Davidson (*12*, p. 186),

> Twenty-five minutes after the great eruption, a great "earthquake wave," estimated as from twenty-five to thirty feet high, came upon Port Graham [near English Bay] like a wall of water. It carried off all the fishing-boats from the point, and deluged the houses. . . . Fortunately it was low water, or all of the people at the settlement must inevitably have been lost. The tides rise and fall about fourteen feet.

An annual report of the Russian Orthodox Missionary at Kenai dated 28 May 1884, also makes a similar reference to the waves generated by the eruption at Alexandrovsky (Russian name for English Bay) (*13*). "This region suffered from inundation caused by

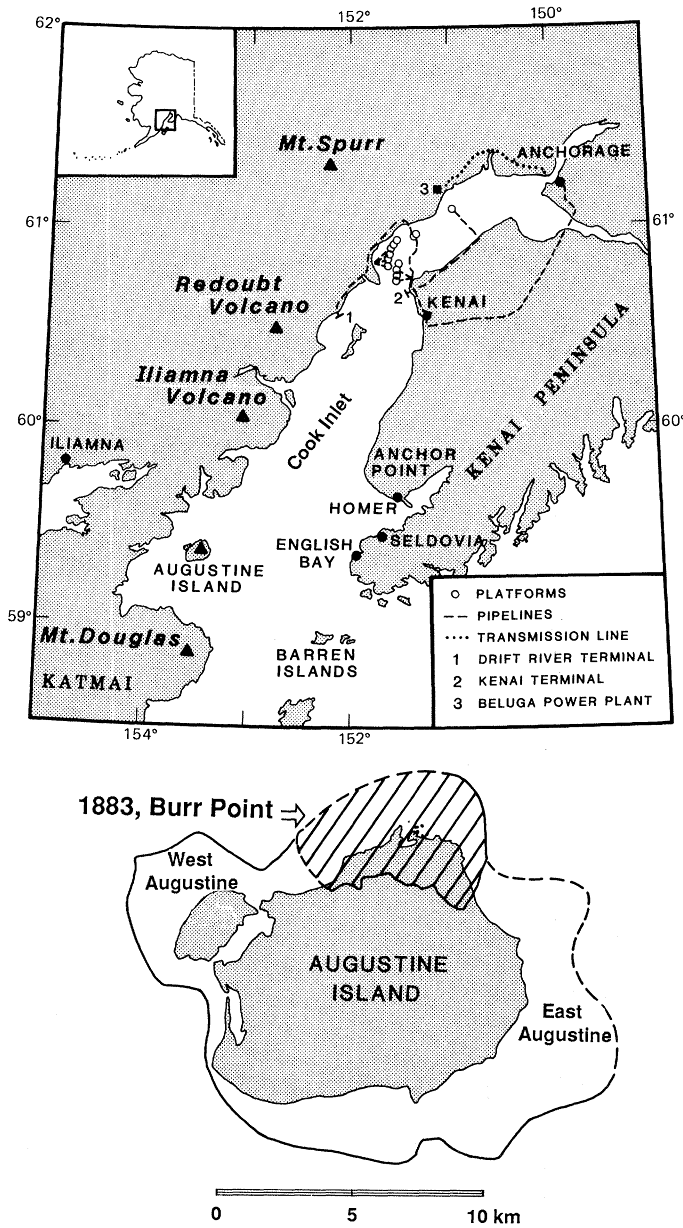

Fig. 1. (**Top**) Location of Mount St. Augustine and Cook Inlet settlements, oil production platforms, and pipelines. (**Bottom**) Mapped offshore debris avalanches. Few have been dated: the east avalanche has a minimum carbon age of 1500 before the present. The west Augustine debris avalanche is much younger. The Burr Point avalanche is historic and was emplaced on 6 October 1883; it covers an area of about 25 km^2.

the eruption of Chernabura Volcano which is about 60 miles across strait from Alexandrovsky."

A narrative of the 1883 eruption that makes reference to large sea waves near St. Augustine Island during the eruptions comes from a recently discovered field notebook from 1898 of the pioneering U.S. Geological Survey geologist J. A. Spurr (*14*).

> Trader says here at Katmai that eighteen years ago three families from Kodiak went with families and baidarkas to St. Augustine Island to spend the winter . . . the mountain began to shake so violently that they put all their effects in their baidarkas and started on a stormy day. Scarcely were they at the mouth of the bay when an explosion occurred, ashes, boulders and pumice began pouring down and the barabaras were buried and the bay filled up with debris. At the same time there were many tidal waves, so that the natives nearly perished with fright, yet finally escaped.

New detailed bathymetry (*15*) clearly shows a major offshore lobe of the typical hummocky terrain that characterizes the surface of avalanche deposits at the north side of St. Augustine Island. This debris avalanche lobe was formed in 1883, as confirmed by field studies in 1986 (*16*), and extends at least 3 km offshore (Fig. 1, bottom). Onshore, at Burr Point, the hummocky 1883 surface of the debris avalanche has been smoothed out by subsequent pyroclastic flows. However, the pre-1883 shoreline can still be identified fairly easily today; we have sketched it in on Fig. 1, bottom. Figure 1 also shows other young offshore debris avalanches that can be recognized on the new bathymetric map. Each one of these avalanches could have produced a tsunami. Figure 2 (top) is a sketch of Mount St. Augustine made in 1870 that shows the volcano from the north side before edifice collapse (*17*); Fig. 2 (bottom, 1909 photograph) shows the horseshoe-shaped depression at the volcano's summit, created by edifice collapse in 1883. Subsequent to collapse, the depression was partially filled by a new dome that was extruded at the end of the 1883 eruptive cycle.

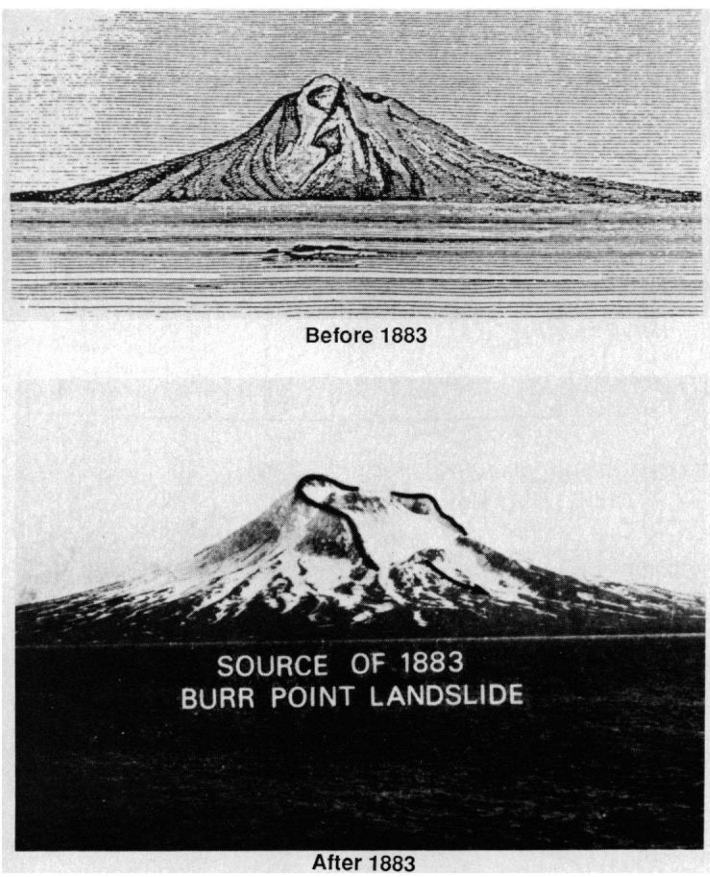

Fig. 2. Source area of 6 October 1883 Burr Point debris avalanche, which left a 0.7-km-wide, horseshoe-shaped crater, open to the north. (**Top**) Sketch of Mount St. Augustine as seen from the northeast, before 1883 (*17*). (**Bottom**) Photograph taken from the northeast in 1909, showing the horseshoe crater created on 6 October 1883. The dome and spine occupying the crater before 1883 were presumably removed by the Burr Point debris avalanche and then replaced by a new dome toward the end of the 1883 eruptive cycle.

Need for Numerical Simulation

Because of Mount St. Augustine's history of repeated edifice collapse on virtually all flanks of the volcano, the historic tsunami of 1883, and the present oversteepened configuration of the volcano, there was considerable concern during the 1986 eruptive cycle that the volcano might collapse again, resulting in a tsunami with potentially dangerous wave run-up at Lower Cook Inlet coastal communities (*7, 8*). Judging from the 6 October 1883 event, low-lying areas along the eastern shore of Lower Cook Inlet from Clam Gulch south (Ninilchik, Happy Valley, Anchor Point, Homer, Seldovia, Port Graham, and English Bay) could expect run-ups of 5 m or more in the event of edifice collapse at Mount St. Augustine. The exact run-up depends on local shoaling of the sea floor. Such waves could take many lives and cause substantial property damage. Homer (population 4000) is the largest of these Lower Cook Inlet communities; its low-lying glacial spit enjoys heavy summer recreational use and is especially vulnerable to large sea waves. There would not be much warning if a tsunami originated at Mount St. Augustine. (Tsunami transit time depends on water depth. The velocity of tsunami propagation is $c = (gH)^{1/2}$, where g is the acceleration of gravity and H the water depth.) A tsunami generated at St. Augustine Island would reach the nearest settlement in as little as 1 hour.

Models

We developed two numerical models. The first uses a regular numerical grid in spherical polar coordinates and covers Lower Cook Inlet from 59° to about 60° N (Fig. 1, top). This area includes all the communities that may be threatened by a tsunami from Mount St. Augustine. The second model uses an irregular triangular grid and includes all of Cook Inlet up to the Anchorage area. This second model, because it covers the entire inlet, allows us to estimate arrival times and wave heights not only of the initial critical set of waves, but also of later-arriving waves produced by reflections at various points along the inlet's shoreline.

Generation and propagation of the tsunami were calculated by using a set of equations of motion and continuity that describe long-wave propagation on the rotating earth. Initial calculations showed little difference in the results when we used nonlinear advective terms in the equations compared to the advection-free equations. Hence, in all subsequent calculations, advective terms were neglected in the equation of motion.

The equations of motion and continuity in a spherical polar coordinate system are (*18*)

$$\frac{\partial U}{\partial t} - fV = - \frac{g}{R \cos \phi} \frac{\partial \eta}{\partial \lambda} - \frac{rUW}{H} \quad (1)$$

$$\frac{\partial V}{\partial t} + fU = - \frac{g}{R} \frac{\partial \eta}{\partial \phi} - \frac{rVW}{H} \quad (2)$$

$$\frac{1}{R \cos \phi} \left[\frac{\partial}{\partial \lambda}(HU) + \frac{\partial}{\partial \phi}(HV \cos \phi) \right] = \frac{\partial \zeta}{\partial t} - \frac{\partial \eta}{\partial t} \quad (3)$$

where λ is east longitude, ϕ is north latitude, R is the radius of the earth, f is the Coriolis parameter, g is gravity, $H(\lambda, \phi)$ is the water depth in the equilibrium state, η is the deviation of the free surface from the equilibrium level, ζ is the bottom displacement, U and V are the east and north components of the depth-averaged current, t is time, r is a bottom friction coefficient, and $W = (U + V)^{1/2}$. As for the boundary conditions, a radiation condition was used at the open boundaries, and at the shores the normal velocity component was assumed to be zero.

The grid and the finite-difference equations used in the first model are similar to those used by Ramming and Kowalik (*19*). The model has been applied to earthquake-generated tsunamis in the Gulf of Alaska (*20*). The regular grid used to model only Lower Cook Inlet has a spacing of 2 minutes in the longitudinal direction and 1 minute in the latitudinal direction. At latitude 60°, both distances are equal to 1 nautical mile (1.852 km).

To model the entire Cook Inlet we used the irregular triangular grid shown in Fig. 3, which uses smaller triangles for the coastal shallow regions and larger triangles for deeper water. For the numerical integration in time, we used a finite-difference scheme similar to that developed by Thacker *et al.* (*21*) for triangular grids. Since this model covers all of Cook Inlet, wave height predictions could be made for the city of Anchorage, the largest population center in the inlet. The irregular triangular grid has the advantage over the regular grid of a more efficient use of the computer capacity. Since grid spacing varies with water depth, fewer grid points are needed to represent the bathymetry adequately. Therefore, the program allows a look at the long travel time history of the tsunami (up to 12 hours after the instant of tsunami generation), compared to only 2 hours for the regular grid model.

Results of Computations

Regular grid model (only Lower Cook Inlet). Two cases of debris avalanche–generated waves were studied by using the regular grid model. In the first case, the landslide was assumed to enter the sea at Burr Point at the northern shore of St. Augustine Island, as in 1883. The area of the 1883 slide was computed at 25 km^2 from the bathymetric map (*15*). The advance of the avalanche along the sea floor was simulated as a progressive 25-m uplift of the sea floor, propagating from the shore to the open sea at a speed of 50 m/sec. This value was estimated from observed and theoretically calculated velocities for the first Mount St. Helens rockslide avalanche of 18 May 1980 (average velocity, 35 m/sec; peak velocity, 70 m/sec), and from theoretical velocities calculated for Mount St. Augustine debris avalanches (*22*). In the second case, a debris avalanche was assumed to enter the sea at the eastern shore of St. Augustine Island where several prehistoric debris avalanches have been mapped offshore (*15*) (Fig. 1, bottom). The purpose of the two numerical simulations were (i) to calculate the tsunami travel times to various coastal locations, (ii) to estimate wave amplitudes at critical locations, and (iii) to study the directional properties of the landslide-generated waves.

Figure 4 shows three-dimensional snapshots of the propagating tsunami generated at Burr Point in 1883. The pictures show the tsunami at various times after debris avalanche impact. Calculations are based on the regular grid model. The vertical scale varies from plot to plot; for reference, the small step used to indicate the shoreline is 25 cm high. On each plot, maximum wave heights attained are also annotated. One can see the outward propagation of the tsunami from the northern shore of St. Augustine Island; it is faster in the deep water to the north-northeast, slower on the shallow shelf to the south of the island. Arrival of the tsunami in

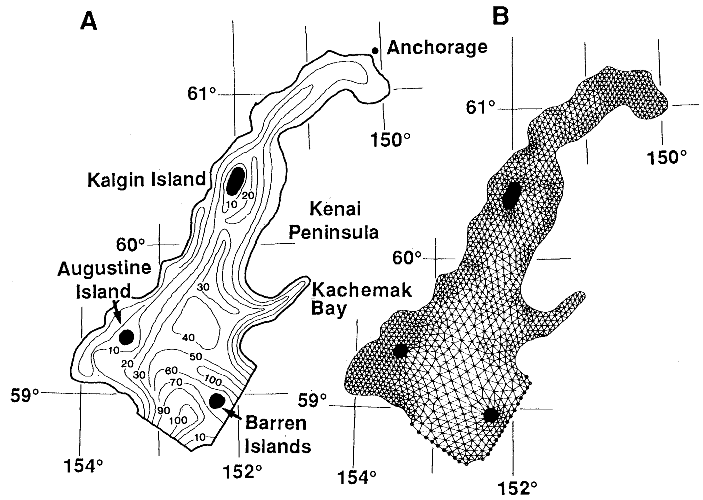

Fig. 3. (**A**) Bathymetry of Cook Inlet in fathoms. (**B**) Irregular triangular grid used to approximate water depths in the computations.

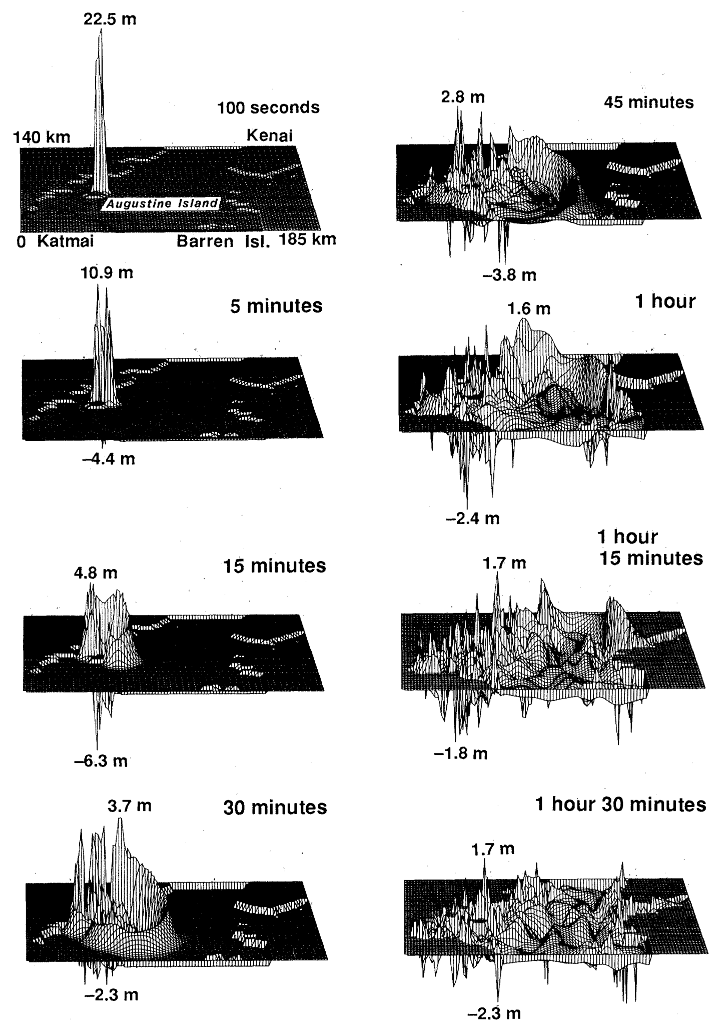

Fig. 4. Numerical regular grid model of long-wave propagation for 1883 Mount St. Augustine tsunami. Snapshots of the propagating tsunami at various time intervals after impact of the Burr Point debris avalanche at the northern shore of St. Augustine Island. Vertical scale varies from frame to frame: the shoreline is shown as a 25-cm-high step. The source was modeled as an incremental 25-m uplift of the sea floor in three successive steps, simulating an advancing avalanche across the sea floor at 50 m/sec. Source area is 25 km^2.

narrow bays results in a strong amplification of the waves. Generally, tsunami amplitude decreases with distance from St. Augustine Island, but amplitudes increase again when the tsunami reaches the shoaling shorelines of Cook Inlet. Turbulent seas produced by constructive and destructive interference of reflected waves can be best seen in the last two frames (1 hour 15 minutes and 1 hour 30 minutes). Figure 5A summarizes these results as contours of tsunami travel time across Lower Cook Inlet. The contours indicate the arrival of the first wave as it reaches 1 cm in amplitude.

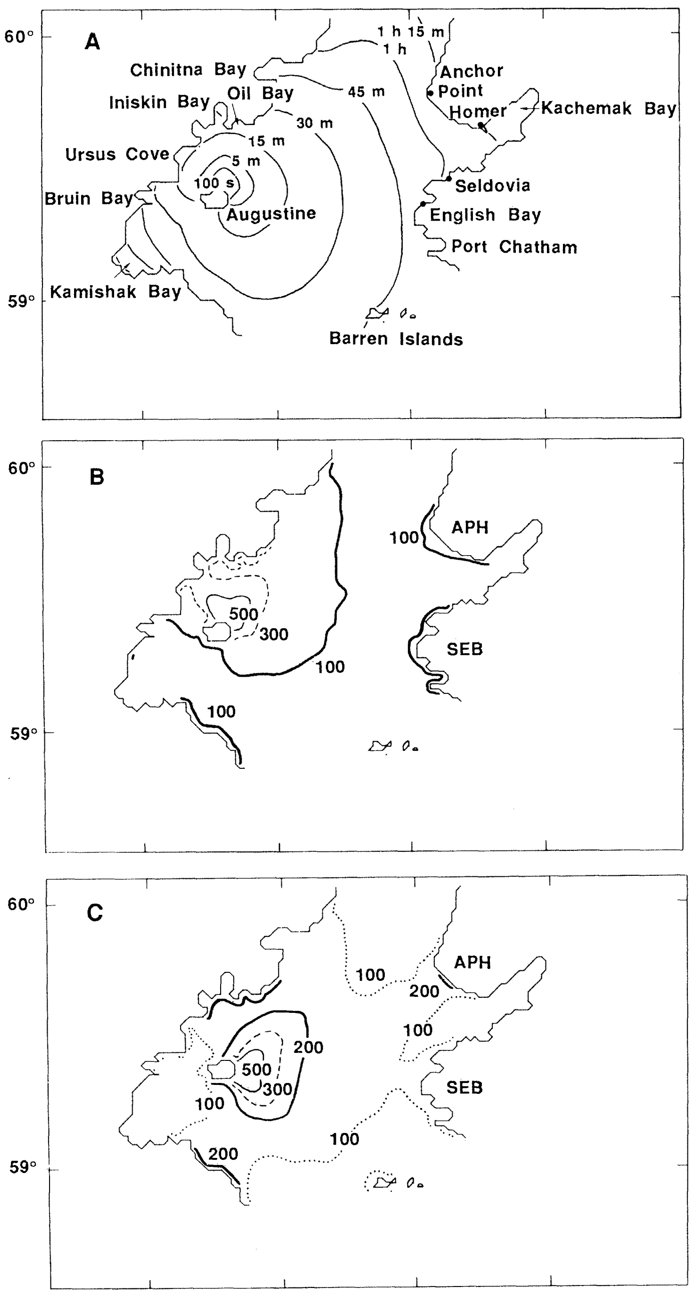

Fig. 5. (**A**) Tsunami travel times from Mount St. Augustine to Lower Kenai Peninsula settlements for impact of a debris avalanche at the northern shore of Augustine Island. Abbreviations: s, seconds; m, minutes; and h, hour. Adapted from (*8*) with permission (copyright by American Geophysical Union). (**B**) Maximum amplitude calculations (in centimeters) for debris avalanche impact at the northern shore of St. Augustine Island. Abbreviations: APH, Anchor Point–Homer; and SEB, Seldovia–English Bay. (**C**) Same calculation as for (B) for impact at the eastern shore. For both (B) and (C), impacts occur over an area of 25 km^2 with a forward velocity of the debris avalanche of 50 m/sec.

The spatial distribution of tsunami energy depends on the properties of the tsunami source (*23*). In order to compare the directional properties of the tsunamis resulting from the two modeled landslides, the maxima of tsunami amplitudes were plotted for each case. The maximum is found by picking the largest amplitude at each grid point during the tsunami propagation window (2 hours). Figure 5, B and C, shows contours of maximum wave heights for debris avalanches striking the sea at the northern and eastern shores of St. Augustine Island. Because of wave reflections from the island's shoreline, the energy is directed mainly to the north-northeast for north shore impact and mainly to the east for the east shore impact. In both cases, the amplitude of the tsunami on the Lower Kenai Peninsula is not uniform; there are regions of larger-than-average wave amplitudes along the Anchor Point–Homer (APH) shoreline and along the Seldovia–English Bay (SEB) shoreline (Fig. 5, B and C).

To confirm this wave pattern, the distribution of maximum water particle velocity in the oscillatory wave was also calculated based on the magnitude of the depth-averaged current $W = (U + V)^{1/2}$. For eastern impact, region APH experiences anomalously high wave velocities, as high as 200 cm/sec. Velocities greater than 100 cm/sec are found for region SEB. A similar picture was obtained for northern impact. Thus, both the maximum potential energy and the maximum kinetic energy of the waves show similar distributions. These patterns are clearly related to the well-known oceanographic phenomenon of wave energy concentrations around peninsulas by refraction.

Irregular grid model (all of Cook Inlet). The irregular triangular grid model, because it includes the bathymetry for all of Cook Inlet, yields answers to several questions that the regular grid model could not resolve. Although the direct wave contains most of the wave energy and is largest in amplitude, secondary waves produced by reflections at various points of the Cook Inlet shoreline can also have large amplitudes. By using the irregular grid model, we can study the complete time history of the tsunami, including the reflected wave trains. Figure 6, A and C, shows sea level fluctuations at English Bay for the 1883 tsunami model (northern impact). Figure 6A covers a 3-hour window after wave generation (regular grid); Fig. 6C covers an 8-hour window (irregular grid). The wave amplitudes are calculated for grid points close to English Bay (Fig. 5A), but, because of the different constructions of the regular and irregular grids, the points at which the wave amplitudes were calculated are not exactly identical. Figure 6, B and D, shows a similar pair of wave amplitude calculations for Homer.

Comparison of wave amplitudes at English Bay and Homer for the two different models shows good agreement of the overall wave pattern. The plots calculated for the irregular grid model show interesting late-arriving reflected wave trains with relatively large amplitudes. Relatively high amplitude waves arrive from the head of the inlet up to 8 hours after the instant of tsunami generation.

A tsunami generated at the northern shore of St. Augustine Island as in 1883 would propagate to Anchorage in about 4 hours, but the shallows of Upper Cook Inlet would greatly attenuate the waves (Fig. 6E).

Discussions and Conclusions

The results of both the regular and the irregular grid models are in imperfect but plausible agreement with on-site observations at English Bay on 6 October 1883. Calculated peak amplitudes for the first wave are 1.8 m for the regular grid model and 1.3 m for the irregular grid model. The author of the daily log (*10*) that was kept by the Alaska Commercial Company at English Bay estimated the

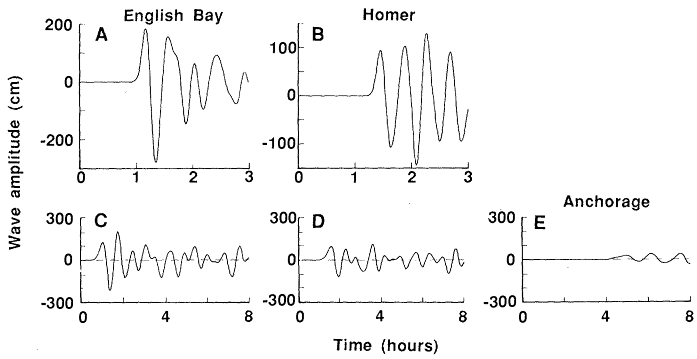

Fig. 6. Wave amplitudes at English Bay (**A** and **C**), Homer (**B** and **D**), and Anchorage (**E**). For (A) and (B) we used regular grid models; for (C), (D), and (E), irregular grid models.

rise of the sea "above the usual level" at 20 feet (6.1 m). Davidson (*12*) reported a similar estimated wave height of the first-arriving wave of 25 to 30 feet (7.6 to 9.1 m). Our wave height calculations are lower by a factor of 3 to 7 than both of these observations. There are four reasons that could account for this discrepancy. (i) The initial wave height at Burr Point on St. Augustine Island was taken as 25 m, which is a conservative value judging from heights of water waves associated with historical landslides (*24*). Since the wave equations are linear, doubling of the initial wave height would also double the final amplitude. (ii) The predicted wave amplitudes would increase substantially if we accounted in detail for the shoaling of the sea bottom at English Bay by using a finer computational grid. (iii) Our estimate of the impact velocity of the debris avalanche might be too low, and (iv) the wave amplitudes observed in 1883 may have been overestimated.

Tsunami travel time from Mount St. Augustine to English Bay is 63 minutes. The error could certainly not be more than 10%, ± 6 minutes. An unresolved problem is whether the first explosion heard at about 0800 on 6 October 1883 (*12*) was related to edifice collapse that caused the ensuing tsunami. The 18 May 1980 Mount St. Helens eruption is an example of how explosive eruptive activity was triggered by unloading of the edifice by a landslide. In this case, a very shallow magma intrusion (cryptodome) was responsible for the great bulge, 2 km in diameter and 100 m in amplitude, that developed on the high northern flank of Mount St. Helens before the events of 18 May. Unloading of this magma intrusion by edifice collapse resulted in a sudden vesiculation of the intrusion, producing a horizontal blast at the moment when the debris avalanche fell away from the mountain (*25*). If we apply this scenario to Mount St. Augustine, that is, if the first audible explosion followed edifice collapse within seconds, the tsunami should have arrived at English Bay at 0900 to 0902. This estimate accounts for the travel time of sound across Lower Cook Inlet (4 to 5 minutes) and the time for the debris avalanche to reach the sea (2 to 3 minutes). However, observers at English Bay reported arrival of the tsunami at 0815 to 0825. Hence there is a half- to three-quarter–hour difference between the expected and observed tsunami arrival times. Possible explanations for the discrepancy are that (i) the reported 25-minute time difference between sound and tsunami arrival times was incorrect (estimates by Davidson and the Alaska Commercial Company of the actual time of tsunami arrival differ by 10 minutes) and (ii) the tsunami was triggered by edifice collapse 30 to 45 minutes before the onset of recognized explosive activity.

The tsunami models presented in this article do not take into account tidal fluctuations in Cook Inlet, which are as high as the wave amplitude calculated for the 1883 event. If the tsunami occurs at low tide, as on 6 October 1883, the hazard is not very great. However, if it occurs at high tide, low-lying areas of Lower Cook Inlet coastal communities are in great danger of being overrun. The short time between tsunami generation near the volcano and arrival at Lower Cook Inlet towns presents a challenge to devising an effective warning system.

From a practical point of view, the calculations presented here were useful for emergency planning during the 1986 Mount St. Augustine eruptive crisis. Although this work was site-specific, the potential hazard of a tsunami—and the potential use for such modeling endeavors—is not. A significant tsunami hazard exists near many coastal volcanos in the circum-Pacific regions of Alaska, Kamchatka, the Kurile Islands, Japan, the Philippines, Indonesia, and Papua New Guinea, as well as in other areas with volcanos near the coast, for example, the Mediterranean region or the West Indies.

REFERENCES AND NOTES

1. J. H. Latter, *Bull. Volcanol.* **44**, 467 (1981).
2. T. Simkin and R. S. Fiske, *Krakatau 1883* (Smithsonian Institution, Washington, DC, 1983), p. 219.
3. L. Siebert and J. Kienle, abstract, International Volcanology Congress, International Association of Volcanology and Chemistry of the Earth's Interior, New Zealand, February 1986; L. Siebert, *J. Volcanol. Geotherm. Res.* **22**, 103 (1984); T. Ui, *ibid.* **18**, 135 (1983); _____, H. Yamamoto, K. Suzuki-Kamata, *ibid.* **29**, 231 (1986).
4. L. Siebert, H. Glicken, T. Ui, *Bull. Volcanol.*, in press.
5. I. Aida, *J. Seismol. Soc. Jpn.* **28**, 449 (1975).
6. The submarine explosion is described by G. I. Yokoyama [*J. Volcanol. Geotherm. Res.* **9**, 359 (1981)]; R. D. M. Verbeek, *Krakatau* (Krakatau Government Press, Batavia, 1885); S. Self and M. R. Rampino, *Nature (London)* **294**, 699 (1981); G. Camus and P. M. Vincent, *J. Volcanol. Geotherm. Res.* **19**, 167 (1983). Edifice collapse is described by J. W. Francis and S. Self [*Sci. Am.* **249**, 172 (November 1983)]. Emplacement of pyroclastic debris is described by J. H. Latter [in (*1*)]. Collapse followed by explosion is described by P. W. Francis [*J. Volcanol. Geotherm. Res.* **25**, 349 (1985)].
7. J. Kienle, *Eos* **67**, 172 (1986).
8. _____, J. N. Davies, T. P. Miller, M. E. Yount, *ibid.*, p. 582.
9. J. Kienle and S. E. Swanson, "Volcanic hazards from future eruptions of Augustine Volcano, Alaska" (UAG R-275, Geophysical Institute, University of Alaska, Fairbanks, ed. 2, 1985).
10. Log book from the Alaska Commercial Company Records, in Alexandrovsky, in 1883 (University of Alaska Archives, Fairbanks).
11. Chonoborough is a local version of the Russian name (Ostrov) Chernoburov, meaning "black-brown" (island), according to D. J. Orth [*U.S. Geol. Surv. Prof. Pap. 567* (1967), p. 93]; some spellings found in the literature are Chernobur, Chernobour, Chernoborough, Chernaboura, and Tchernybura.
12. G. Davidson, *Science* **3**, 186 (1884).
13. Russian Orthodox Missionary at Kenai, *Annual Report, 1884* (University of Alaska Archives, Fairbanks).
14. The occupation and evacuation of St. Augustine Island by these families is also mentioned by Davidson (*12*); the eruption must have been that of 6 October 1883, rather than 1880, as suggested by J. A. Spurr's reference to "18 years ago" as related by the trader. J. A. Spurr's 1898 field notebook is now in the U.S. Geological Survey archives in Menlo Park, CA.
15. Hydrographic survey H-9073 was performed by the National Oceanic and Atmospheric Administration–National Ocean Survey in the vicinity of St. Augustine Island, and was contoured in 1978 by J. Whitney, then at the U.S. Geological Survey Conservation Division in Anchorage.
16. L. Siebert, H. Glicken, J. Kienle, *Eos* **67**, 1259 (1986).
17. P. Doroshin, *Verhandlungen der Russisch-Kaiserlichen Mineralogischen Gesellschaft zu St. Petersburg* (Kaiserliche Mineralogische Gesellschaft, 1870), series 2, vol. 5, p. 25 (in Russian).
18. T. S. Murty, *Storm Surges—Meteorological Ocean Tides* (Bulletin 212, Fisheries Research Board of Canada, Ottawa, 1984), p. 44.
19. H. G. Ramming and Z. Kowalik, *Numerical Modelling of Marine Hydrodynamics* (Elsevier, New York, 1980), p. 148.
20. Z. Kowalik and T. S. Murty, *Geophys. Res. Lett.* **11**, 1243 (1984).
21. W. C. Thacker, A. Gonzales, G. E. Putland, *J. Comput. Phys.* **37**, 371 (1980).
22. B. Voight, R. J. Janda, H. Glicken, P. M. Douglass, *Geotechnique* **33**, 243 (1983); B. Voight, *U.S. Geol. Surv. Prof. Pap. 1250* (1981), p. 85, figure 47; J. Beget, unpublished theoretical estimates of debris avalanche velocities as a function of distance from the summit of Mount St. Augustine, showing that at the distance where the 1883 Burr Point avalanche entered the sea the velocity was 90 m/sec, decelerating to about 50 m/sec at the terminus of the avalanche.
23. A. Zielinski and N. K. Saxena, *Sci. Tsunami Hazards* **2**, 113 (1984).
24. R. L. Slingerband and B. Voight, in *Engineering Sites*, vol. 2 of *Rockslides and Avalanches*, B. Voight, Ed. (Elsevier, New York, 1979), p. 356.
25. R. Decker and B. Decker, *Sci. Am.* **244**, 68 (March 1981); R. L. Christiansen and D. W. Peterson, *U.S. Geol. Surv. Prof. Pap. 1250* (1981), p. 17.

26. Supported by National Science Foundation (NSF) grants EAR-8612283 and EAR-8612274 (J.K.) and ECE-8414747 (Z.K.). We thank J. A. Maccini and J. L. Snyder of NSF for providing emergency funds; C. Chu for help with the three-dimensional computer plots; C. Helfferich for assistance with the manuscript; and V. Alexander, J. Beget, L. Gedney, C. Newhall, J. Niebauer, L. Siebert, and D. Stone for reviewing the manuscript.